Study of Compressed Sensing Algorithms for Highly Coherent Systems

A Project Report

submitted by

JAYASOORYA K. E.

in partial fulfilment of the requirements
for the award of the degree of

MASTER OF TECHNOLOGY

DEPARTMENT OF ELECTRICAL ENGINEERING
INDIAN INSTITUTE OF TECHNOLOGY MADRAS.

June 2017

THESIS CERTIFICATE

This is to certify that the Project Report titled **Study of Compressed Sensing Algorithms for Highly Coherent Systems**, submitted by **Jayasoorya K. E., EE15M069**, to the Indian Institute of Technology, Madras, for the award of the degree of **Master of Technology**, is a bona fide record of the research work done by her under my supervision. The contents of this report, in full or in parts, have not been submitted to any other Institute or University for the award of any degree or diploma.

Dr. Sheetal Kalyani
Project Guide,
Associate Professor,
Dept. of Electrical Engineering,
IIT Madras, 600 036.

Place: Chennai

Date : June 9, 2017

ACKNOWLEDGEMENTS

I would like to take this opportunity to extend my sincere gratitude to my guide Dr. Sheetal Kalyani for her continuous support and guidance. I am indebted to her for the encouragement I received to pursue research. I earnestly thank her for her invaluable advices and immense support throughout my project.

I would like to extend my thanks to Sreejith and other PhD scholars under Dr. Sheetal Kalyani for helping me out throughout the project. Without them I wouldn't have been able to complete the project.

Finally, I would like to thank my parents and friends for their support all these years of my life.

ABSTRACT

KEYWORDS: Coherent systems, Generalized Space Shift Keying, Compressed Sensing, SWAP, multiple input multiple output, Kronecker channel

Accurate estimation of a sparse vector in a high dimensional linear regression problem using small number of measurements or compressed sensing (CS) has attracted considerable attention in the past few years. Compressed sensing based sparse recovery techniques are widely used for variety of applications. Here we are considering the application of CS to generalized space shift keying (GSSK) detection. GSSK is an emerging multiple input multiple output (MIMO) technique which uses antenna indices to transmit information. However, none of the existing GSSK detection algorithms take into account the significant correlation present in practical MIMO channel models. In this work, we propose a novel framework for improving the performance of existing GSSK detection algorithms in the presence of correlated channels. The proposed framework is based on a modified version of the popular SWAP algorithm. Numerical simulations indicate that the proposed framework can significantly improve the performance of existing CS based GSSK detection schemes with a very modest increase in the computational complexity even when the channel model is highly correlated.

TABLE OF CONTENTS

LIST OF TABLES

LIST OF FIGURES

ABBREVIATIONS

AAI	Active Antenna Indices
ABEP	Average Bit Error Probability
BPDN	Basis Pursuit De-Noising
BE	Band Exclusion
BER	Bit Error Rate
CS	Compressed Sensing
CSR/ CSS	Convex Superset Relaxation/ Selection
GSSK	Generalized Space Shift Keying
ISR	Iterative Sparse Reconstruction
LASSO	Least absolute shrinkage and selection operator
LO	Local Optimization
MAP	Maximum a Posteriori
MIMO	Multiple Input Multiple Output
ML	Maximum Likelihood
NCS	Normalized Compressed Sensing
OMP	Orthogonal Matching Pursuit
ObMP	Oblique Matching Pursuit
QAM	Quadrature Amplitude Modulation
RF	Radio Frequency
RIP	Restricted Isometry Property
SBL	Sparse Bayesian Learning
SM	Spatial Modulation
SNR	Signal to Noise Ratio
SSK	Space Shift Keying
SR	Sparse Reconstruction

i.i.d	Independent and Identically Distributed

NOTATION

$\mathbb{C}$	Set of complex numbers
$\mathbb{R}$	Set of real numbers
$\mathbb{E}$	Probability expectation
$\|\|\mathbf{x}\|\|_p$	l_p norm of $\mathbf{x} \in \mathbb{C}^n$
$\mathbf{A}^T$	Transpose of matrix $\mathbf{A}$
Re$(\mathbf{A})$	Real part of $\mathbf{A}$
Im$(\mathbf{A})$	Imaginary part of $\mathbf{A}$
$\mathbf{I}_n$	Identity matrix $\in \mathbb{C}^{n \times n}$
$\lfloor x \rfloor$	Largest integer less than or equal to x
$x[n]$	n^{th} sample of the vector observation **x**
$\mathcal{N}(\mu, \sigma^2)$	Normal random variable with mean μ and variance σ^2
$\mathcal{CN}(\mathbf{0}, \sigma^2\mathbf{I}_n)$	Zero mean complex Gaussian random vector (R.V) with covariance $\sigma^2\mathbf{I}_n$
$\sim$	Distributed as, for example, $X \sim \mathcal{N}(0,1)$ denotes X is a zero mean Gaussian random variable with variance 1
$\|\mathcal{I}\|$	Cardinality of set $\mathcal{I}$
vec(•)	Operator that stacks the columns of a matrix into one tall vector
tr(•)	The sum of the diagonal elements of a matrix or the trace of a matrix
$\odot$	element-wise product of two matrices
$\langle \bullet, \bullet \rangle$	Inner product

CHAPTER 1

Introduction

Compressed sensing (CS) is a signal acquisition paradigm that has gained popularity in recent years. CS enables the recovery of a high dimensional sparse signal in an under-determined system where the number of observations are much less compared to the dimension of the unknown signal. Some of the standard CS techniques include LASSO, Orthogonal Matching Pursuit (OMP), Compressive Sampling Matched Pursuit (CoSaMP), etc. These algorithms perform well when the columns of the measurement matrices are uncorrelated. However most of the practical problems involve measurement matrices with a structured or non-structured statistical dependency existing between columns.

Extensive work has been done till date for analyzing the performance of the sparse recovery procedure with highly coherent measurement matrices. The existing theory in CS for uncorrelated measurement matrices is extended to observation matrices that exhibit structured statistical dependencies across its rows and columns in [1]. The specific example of random Toeplitz matrices is considered for illustration, which arise naturally from the convolutional structure inherent to linear system identification problems. In [2], the limiting laws of the coherence of an $n \times p$ random matrix in the high-dimensional setting where p can be much larger than n are derived. Some works shows the upper bound on mutual coherence values above which algorithms like OMP fails to recover the unknown sparse signal.

Besides these theoretical works, modifications in existing algorithms are done in order to improve the performance when subjected to coherent measurement matrices. In [3, 4], the authors have described modifications in the well known low complexity algorithm OMP to cope up with the coherence in measurement matrices.

Novel techniques like band exclusion (BE) and Local optimization (LO) are proposed in [5], which can be applied to algorithms like OMP, Subspace Pursuit (SP), Iterative Hard Thresholding (IHT), Basis Pursuit (BP) and LASSO, and result in the

modified algorithms BLOOMP, BLOSP, BLOIHT, BP-BLOT, and LASSO-BLOT, respectively.

Development of new algorithms which address the problem of coherence in design matrices are dealt with in [6–8]. The Sparse Bayesian Learning (SBL) algorithms proposed in [6] are widely popular for their superior recovery performance especially in the presence of high temporal correlation.

A simple greedy algorithm, called SWAP, that iteratively swaps variables until convergence is described in [9]. SWAP is proved to output the true support, the locations of the non-zero entries in the sparse vector, under a relatively mild condition on the measurement matrix. SWAP can also be used to boost the performance of any sparse regression algorithm.

One of the widely popular method of dealing with coherent dictionaries is clustering [10, 11]. The correlated variables are clustered first using clustering algorithm based on canonical correlations. Subsequently sparse estimation such as the LASSO for cluster-representatives or the group LASSO based on the structure is applied in [10]. Similar method is adopted in [11] whereas a clustering removal algorithm is proposed in [12].

Some of the applications where these algorithms are applied are MIMO detection with correlated channel, denoising and compression, fMRI (functional Magnetic Resonance Imaging), gene expression data analysis, discretization of continuum imaging problems such as radar and medical imaging, super resolution of images etc. Here we are taking the specific example of detector design for correlated channels in generalized space shift keying (GSSK).

GSSK, a special technique based on spatial modulation (SM), is a widely used multiple input multiple output (MIMO) index modulation technique. GSSK modulation exploits inherent fading in wireless communication to provide better performance over conventional amplitude/phase modulation (APM) techniques. Spatial modulation uses APM techniques, such as PSK and quadrature amplitude modulation (QAM), as well as the antenna index to convey information whereas in each GSSK transmission, only a set of selected antennas transmit signals and the location of such active antennas or active antenna indices (AAI) alone convey information. Since, only few antennas

are active in each transmission, both energy consumption and transmitter complexity in terms of RF circuitry is minimal in GSSK systems when compared to traditional MIMO schemes like spatial multiplexing, space time block coding etc. A fundamental issue in the design of GSSK system is the incredibly high complexity of the optimal maximum likelihood (ML) algorithm. This necessitated the development of suboptimal detection techniques like the compressed sensing (CS) based detection algorithms [13–16], convex superset relaxation (CSR) [17], Gibbs sampling etc. Most of the existing suboptimal schemes assume an uncorrelated channel model. However, in practical large scale MIMO systems, the channel coefficients are found to be highly correlated [18, 19]. Since existing GSSK detection algorithms does not take into account the channel correlation effects, their performance will be highly degraded when applied to real life MIMO channel models with significant correlation.

However, significant contributions are made into analyzing the effect of correlation on the performance of optimal ML detection. In [20], the authors have proposed a general framework based on Moschopoulos method for computing the average bit error probability (ABEP) of SSK- MIMO systems over a generic Rician fading correlated channel with arbitrary parameters. Exact computation of ABEP over generically correlated and non- identically distributed Nakagami m fading channels for the special case of to multiple input single output (MISO) system is reported in [21]. Furthermore, the performance of spatial modulation (SM) systems over arbitrary correlated fading channels is studied in [22].

However, no low complexity GSSK detection algorithm robust to the channel correlation is proposed in open literature to the best of our knowledge. In this work, we propose a novel two stage GSSK detection framework to improve the performance of existing GSSK detection algorithms. In the first stage any CS or non-CS GSSK detection algorithm can be used to produce a preliminary estimate of AAI. This preliminary estimate is latter processed using a novel algorithm called modified SWAP proposed in this work. Modified SWAP, as the name suggests, is developed by modifying the SWAP [9] discussed earlier. The proposed modification to SWAP is based on incorporating the structure in GSSK transmitted vector and has better performance and lower computational complexity in comparison with the original SWAP algorithm. Numerical simulations indicate the superior performance of the proposed two stage GSSK detection framework over existing detection algorithms over a wide range of experiments

involving correlated channel models. Note that this improved performance is achieved without any significant increase in the overall computational complexity.

This thesis is organized as follows:

Chapter 2 discusses the system model of GSSK used in this work. The various channel models used for illustration are also introduced. The Kronecker channel model is briefly described along with the generation of simulated correlated channel coefficients. Various algorithms used for GSSK detection are described along with their performance guarantees and complexities.

Chapter 3 introduces the SWAP algorithm and the proposed modified version. The two stage framework of using modified SWAP in GSSK detection has been described. Complexity of the algorithm is also discussed.

Chapter 4 illustrates the performance of modified SWAP in GSSK detection through numerical simulations. Simulations are done for a range of channel models. Comparisons between various channel models are also illustrated.

Chapter 5 provides some concluding remarks along with avenues for future work.

CHAPTER 2

GSSK System Model and Detection Algorithms

2.1 GSSK System Model

We consider a MIMO system with N_t number of transmit antennas and N_r number of receive antennas. Figures 2.1 and 2.2 shows the System model of GSSK. [23] The MIMO model is given by

$$\mathbf{y} = \mathbf{H}\mathbf{x} + \mathbf{n}, \tag{2.1}$$

where $\mathbf{H}$ represents the channel matrix, $\mathbf{y}$ is the received signal, $\mathbf{x}$ and $\mathbf{n}$ are transmitted symbol and noise respectively. Channel matrix $\mathbf{H}$ is assumed to be known at the receiver. The noise vector $\mathbf{n}$ is distributed as $\mathcal{CN}(\mathbf{0}, \sigma^2\mathbf{I}_{N_r})$. In a GSSK system with n_t active antennas the transmitted symbol $\mathbf{x}$ will have 1 in n_t locations corresponding to the active antennas and 0 in the rest $N_t - n_t$ locations. Let $\mathcal{I} = \{i : \mathbf{x}_i = 1\}$ represents the active antenna indices (AAI) in a particular transmission. $\mathcal{I}$ contains the complete information in transmitted signal. This GSSK system can achieve a spectral efficiency of $S = \left\lfloor \log_2 \left(\binom{N_t}{n_t} \right) \right\rfloor$ bits/s/Hz and has 2^S valid transmitted symbols [13]. Most of the works consider a channel model where each entry in $\mathbf{H}$ is *i.i.d* sampled from a $\mathcal{CN}(0, 1)$ distribution. However, this model of channel, though widely popular in MIMO literature, does not reflect the true propagation characteristics. Significant correlation can exist between individual channel gains. In this article, we consider two channel models which capture this correlation.

2.1.1 Channel Model 1: $\mathbf{H}$ with correlated columns and independent rows.

This is a matrix model widely popular in CS literature. Here, each row of $\mathbf{H}$, i.e., $\mathbf{H}_{i,:}$ is sampled *i.i.d* from a $\mathcal{CN}(\mathbf{0}_{N_t}, \mathbf{\Sigma})$ distribution. The entries in the correlation matrix $\mathbf{\Sigma}$ is given by $\mathbf{\Sigma}_{i,j} = \rho^{|i-j|}$ as introduced in [24], where the parameter $-1 < \rho <$

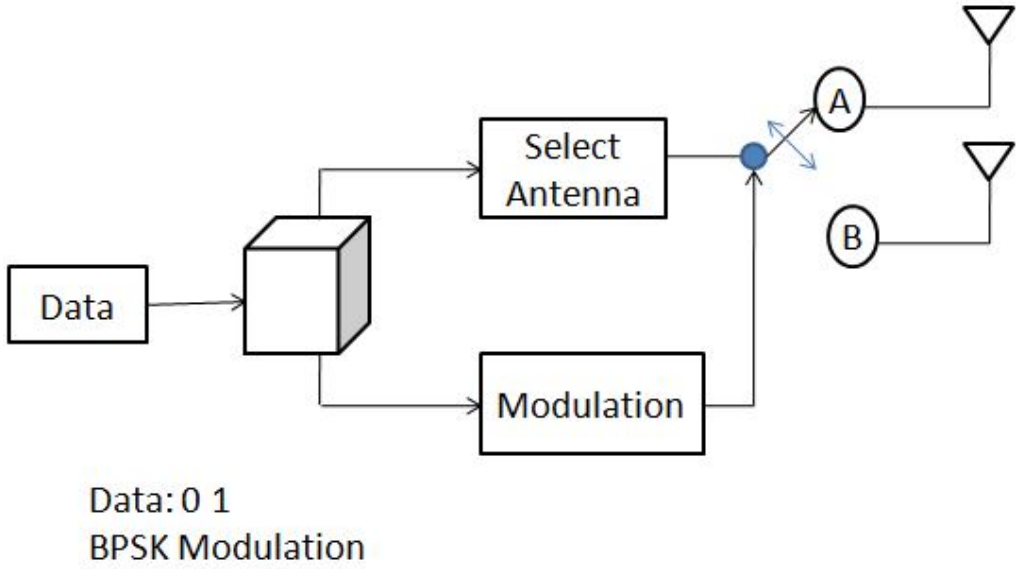

Figure 2.1: Spatial Modulation System Model

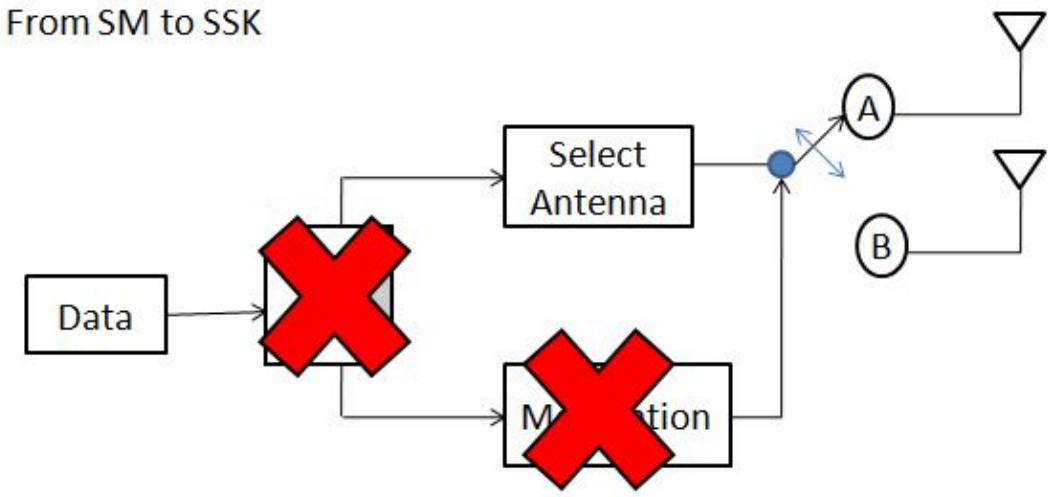

Figure 2.2: GSSK System Model

1 specifies the degree of correlation. As the parameter $|\rho|$ increases, the correlation between columns in $\mathbf{H}$ also increases.

2.1.2 Channel Model 2: Kronecker channel model.

Kronecker model [18] is a widely used MIMO stochastic channel model. One of the main strengths of the proposed MIMO stochastic model is that it relies on a small set of parameters to fully characterize the communication scenario, namely the power gain of the MIMO channel matrix, two correlation matrices describing the correlation properties at both ends of the transmission links, and the associated Doppler spectrum of the channel paths.

For the ease of notations define the $(i,j)^{th}$ entry of channel matrix, i.e., $\mathbf{H}_{i,j}$ by $\alpha_{i,j}$. It is assumed that $\alpha_{i,j}$ is $\mathcal{CN}(0,1)$ distributed.The spatial complex correlation coefficient at the transmitter between antenna m_1 and m_2 is given by

$$\rho^{Tx}_{m_1,m_2} = \langle \alpha_{m_1,n}, \alpha_{m_2,n} \rangle \tag{2.2}$$

(2.2) assumes that the spatial correlation coefficient at the transmitter is independent of j. Similarly, the spatial complex correlation coefficient at the receiver between antenna n_1 and n_2 is given by

$$\rho^{Rx}_{n_1,n_2} = \langle \alpha_{m,n_1}, \alpha_{m,n_2} \rangle \tag{2.3}$$

Finally, the correlation coefficient between two arbitrary transmission coefficients connecting two different sets of antennas

$$\rho^{n_1,m_1}_{n_2,m_2} = \langle \alpha_{m_1,n_1} \alpha_{m_2,n_2} \rangle \tag{2.4}$$

(2.3) assumes that the spatial correlation coefficient at the receiver is independent of m. Using 2.2 and 2.3, one can define the transmitter and receiver correlation matrices $\mathbf{R}_{tx}$ and $\mathbf{R}_{rx}$ as $\mathbf{R}_{tx}(m_1,m_2) = \rho^{Tx}_{m_1,m_2}$ for $1 \leq m_1, m_2 \leq N_t$ and $\mathbf{R}_{rx}(n_1,n_2) = \rho^{Tx}_{n_1,n_2}$ for $1 \leq n_1, n_2 \leq N_r$. So,the spatial correlation matrix of the MIMO radio channel is the Kronecker product of the spatial correlation matrix at the transmitting and receiving ends and is given by

$$\mathbf{R}_{MIMO} = \mathbf{R}_{tx} \otimes \mathbf{R}_{rx} \tag{2.5}$$

where $\otimes$ represents the Kronecker product.

Generation of Simulated Correlated Channel Coefficients

Correlated channel coefficients α_{mn} are generated from zero-mean complex i.i.d., random variables a_{mn} shaped by the desired Doppler spectrum such that

$$\mathbf{A} = \mathbf{Ca} \tag{2.6}$$

where $\mathbb{A}_{MN\times 1} = [\alpha_{11}, \alpha_{12}, ...\alpha_{M1}, \alpha_{M2}...\alpha_{MN}]^T$ and $\mathbf{a_{MN\times 1}} = [\mathbf{a_1}, \mathbf{a_2}, ...\mathbf{a_{MN}}]^{\mathbf{T}}$ where the symmetrical mapping matrix $\mathbf{C}$ results from the standard Cholesky factorization of the matrix $\mathbf{R_{MIMO}} = \mathbf{CC^T}$ provided that $\mathbf{R_{MIMO}}$ is non-singular. Subsequently. the generation of the simulated MIMO channel matrix $\mathbf{H}$ can be deduced from the vector $\mathbf{A}$, as $\mathbf{A} = \mathbf{vec}(\mathbf{H})$.

2.1.3 Channel Model 3: $\mathbf{H}$ with correlated columns and independent rows.

This is a matrix model widely popular in CS literature. Here, each row of $\mathbf{H}$, i.e., $\mathbf{H}_{i,:}$ is sampled *i.i.d* from a $\mathcal{CN}(\mathbf{0}_{N_t}, \mathbf{\Sigma})$ distribution. The entries in the correlation matrix $\mathbf{\Sigma}$ is assumed as a block diagonal matrix given by

$$\mathbf{\Sigma}_{i,j} = \begin{cases} \rho^{|i-j|}, & \text{if } |i-j| \leq \alpha. \\ 0, & \text{otherwise.} \end{cases} \tag{2.7}$$

, where the parameter $-1 < \rho < 1$ specifies the degree of correlation. As the parameter $|\rho|$ increases, the correlation between columns in $\mathbf{H}$ also increases.

2.2 Detection Algorithms

Several algorithms are devised till date for GSSK demodulation. However due to relatively small modulation alphabet detection of GSSK has traditionally been carried out in the optimal maximum likelihood sense [25, 26]. However as the dimension increases,

the maximum likelihood (ML) detector incurs considerable computational complexities. To overcome this issue both optimal and suboptimal schemes are studied in a number of works.

A simple CS framework, Normalized Compressed Sensing (NCS) is described in [13]. The computational complexity is reduced considerably compared to ML. Optimal detection schemes like tree search and column search achieving optimal ML performance are formulated in [17]. In addition, suboptimal detection methods for large MIMO systems and large alphabet GSSK signaling based on convex relaxation, greedy column search, convex superset relaxation (convex superset selection) or CSR (CSS) and semidefinite relaxation (SDR) are also proposed. A low complexity detector is proposed in [27] based on l_∞ minimization having polynomial complexity. In [28], an algorithm called sparse reconstruction (SR) is adopted from image processing to GSSK detection. A modified version of the algorithm, iterative sparse reconstruction (ISR) is also described in the paper.

Several simple modifications of OMP and oblique matching pursuit (ObMP) are formulated in [29]. In particular, maximum a posteriori (MAP) principle has been incorporated to OMP/ObMP so that the posteriori ratio can be maximized iteratively. Due to the fact that the posteriori ratio cannot be evaluated at the receiver unless the activated transmit antennas are known, two types of approximated posteriori ratios are derived. One is a simple approximation that ignores the terms in the posteriori ratio which need the information on transmit antenna activity, and the other is a more complex approximation developed by exploiting the transmit antenna activation probabilities. As a result, two types of MAP-OMPs and MAP-ObMPs are proposed based on these approximations.

The computational complexities of some of the algorithms [13, 15, 17, 28, 29] are given in Table. 2.1

Among the given algorithms ML is optimal, however it is not computationally tractable once the dimension is high. Most of the low complexity algorithms given above do not perform well when the columns of channel matrix $\mathbf{H}$ are correlated. Hence we propose a low complexity GSSK detection algorithm for improving the performance of GSSK detection in correlated channels. The problem statement is explained in the following section.

Computational complexities	
Algorithm	Complexity
ML	$\mathcal{O}(N_r N_t^{n_t})$
NCS with OMP	$\mathcal{O}(n_t N_r N_t)$
NCS with Lasso	$\mathcal{O}(N_t^3)$
CSR	$\mathcal{O}(N_t^3)$
SR	$\mathcal{O}((2N_r)^2 N_t + 2N_t^3)$
ISR (p iterations)	$\mathcal{O}(p((2N_r)^2 N_t + 2N_t^3))$
MMSE	$\mathcal{O}(8N_r^2 N_t)$
ObMP	$\mathcal{O}(N_r^2 N_t)$
MAP1-OMP	$\mathcal{O}(n_t N_r N_t)$
MAP1-ObMP	$\mathcal{O}(N_r^2 N_t)$
MAP2-OMP	$\mathcal{O}(N_t^2 N_r)$
MAP2-ObMP	$\mathcal{O}(N_t^2 N_r)$

Table 2.1: Computational complexities of various algorithms

2.3 Problem statement

We consider the sparse reconstruction of the following problem

$$\mathbf{y} = \mathbf{H}\mathbf{x} + \mathbf{n}, \tag{2.8}$$

as mentioned in 2.1. We define the sparsity of x as the number of non-zero element in x. Thus, the sparse reconstruction of x becomes the estimation of x based on y, H, and the sparsity of x. This problem can be transformed into an l_0-norm minimization problem. However, it is a NP-hard problem.

In [30], Tao and Candes proved that an l_0-norm minimization problem has the same solution as the corresponding l_1- norm minimization problem if restricted isometry property (RIP) condition is satisfied. RIP identifies the constant δ_s of the measure matrix H as the smallest number such that

$$(1 - \delta_s)||x||_2^2 \leq ||Hx||_2^2 \leq (1 + \delta_s)||x||_2^2 \tag{2.9}$$

holds for sparse vector x. If each element of H is an independent Gaussian variable, the matrix H satisfies the RIP with high probabilities. The RIP is to ensure that each pair of columns of H are orthogonal to each other with a high probability.

One commonly used characterization of incoherence in CS is in terms of the mu-

tual coherence μ. Let the pairwise coherence between the kth and jth columns be

$$\mu(k,l) = \frac{\langle a_k, a_l \rangle}{||a_k||||a_l||} \tag{2.10}$$

where a_k and a_l are the column vectors of H.

The mutual coherence of H is the maximum pairwise coherence among all pairs of columns

$$\mu(H) = max_{k \neq l} \mu(k,l) \tag{2.11}$$

Results are shown that if $\mu(H) < \frac{1}{2k-1}$, where k is sparsity of x, then exact support recovery is possible for algorithms like OMP [31].

However when columns of H are correlated the matrix H may not satisfy RIP and hence most of the above algorithms perform poorly when the observation matrix is coherent. In order to improve the performance of these algorithms a novel two stage compressed sensing framework of low complexity is devised here. The framework is explained in the next chapter.

CHAPTER 3

GSSK detection using modified SWAP

In this chapter, we propose a novel two stage GSSK detection framework which is robust to the correlations in the channel matrix. Note that the detection process in GSSK involves the estimation of AAI $\mathcal{I}$ with the aim of minimizing the bit error rate defined by $BER = \mathbb{P}(\hat{\mathcal{I}} \neq \mathcal{I})$. A conversion of the complex MIMO channel model $\mathbf{y} = \mathbf{H}\mathbf{x} + \mathbf{n}$ to its equivalent real form can enhance the detection performance by exploiting the real nature of $\mathbf{x}$ [13–16]. Hence, all the non-ML algorithms discussed in this report are applied to the model $\mathbf{y}_r = \mathbf{H}_r\mathbf{x} + \mathbf{n}_r$, where $\mathbf{y}_r$, $\mathbf{H}_r$ and $\mathbf{n}_r$ represent the real valued entities $\left[\text{Re}(\mathbf{y})^T, \text{Im}(\mathbf{y})^T\right]^T$, $\left[\text{Re}(\mathbf{H})^T, \text{Im}(\mathbf{H})^T\right]^T$ and $\left[\text{Re}(\mathbf{n})^T, \text{Im}(\mathbf{n})^T\right]^T$ respectively. As aforementioned, the BER of detection techniques based on OMP, BPDN, CSR [17] etc. for correlated channels is generally very high in comparison with the performance of same algorithms in uncorrelated channel models. First, we describe an algorithm called SWAP which is known to be robust to correlation in design matrices and a novel modification to the same proposed here.

3.1 SWAP

SWAP is a simple greedy algorithm for sparse regression with correlated measurements [9]. The input to SWAP is an estimate of the support of the unknown sparse vector $\mathbf{x}$, i.e., the location of its non-zero entries. The main idea behind SWAP is to iteratively perturb the estimate of the support by swapping variables. The swapping is done in such a way that a loss function is minimized in each iteration of SWAP. In this way, SWAP seeks to estimate a support, in a greedy manner, that minimizes a loss function. The main reason why SWAP is able to handle correlations is because even if an intermediate estimate contains a variable that is not in the true support, SWAP can swap this variable with a true variable under relatively mild conditions on $\mathbf{H}$.

For any index set $\mathcal{S} \subset \{1, \ldots, N_t\}$ of cardinality $|\mathcal{S}| = n_t$, the authors of [9]

Figure 3.1: Figure shows one iteration of the SWAP algorithm. The shaded region corresponds to the estimate, say $\mathcal{S}(t)$, of the unknown true support that we seek to estimate. The SWAP algorithm swaps a variable i in $\mathcal{S}(t)$ with a variable i' not in $\mathcal{S}(t)$.

considered a loss function of the form

$$\begin{aligned} \mathcal{L}(\mathcal{S}; \mathbf{y_r}, \mathbf{H}_r) &= min_{\alpha \epsilon \mathbb{R}^{n_t}} ||\mathbf{y_r} - \mathbf{H_r}(\mathcal{S})\alpha||_2^2 \\ &= ||\Pi^{\perp}[\mathcal{S}]\mathbf{y_r}||_2^2 \end{aligned} \tag{3.1}$$

where $\mathbf{H}_{\mathcal{S}}$ refers to the $N_r \times |\mathcal{S}|$ matrix that only includes the columns indexed by $\mathcal{S}$ and $\Pi^{\perp}[\mathcal{S}] = \mathbf{I}_n - \Pi[\mathcal{S}]$, $\Pi[\mathcal{S}] = \mathbf{H}(\mathcal{S})(\mathbf{H}(\mathcal{S})^T\mathbf{H}(\mathcal{S}))^{-1}\mathbf{H}(\mathcal{S})^T$

3.1.1 Algorithm and Description

Algorithm 1 SWAP

1: Inputs: Observation $\mathbf{y}_r$, channel matrix $\mathbf{H}_r$ and initial support $\mathcal{S}^{(1)}$
2: Let $r = 1$ and $L^{(1)} = \mathcal{L}(\mathcal{S}^{(1)}; \mathbf{y_r}, \mathbf{H}_r)$
3: Swap $i \in \mathcal{S}^{(r)}$ with $j \in (\mathcal{S}^{(r)})^C$ and compute the loss $L_{i,j}^{(r)} = \mathcal{L}((\mathcal{S}^{(r)}/i) \cup j; \mathbf{y}_r, \mathbf{H}_r)$
4: if $min_{i,j} L_{i,j}^{(r)} < L^{(r)}$ then perform steps 5-7, else, stop.
5: $\{\hat{i}, \hat{j}\} = \arg\min_{i,j} L_{i,j}^{(r)}$ (In case of a tie, choose a pair arbitrarily)
6: Let $\mathcal{S}^{(r+1)} = (\mathcal{S}^{(r)}/\hat{i}) \cup \hat{j}$ and $L^{(r+1)}$ be the corresponding loss.
7: Let r = r + 1 and repeat steps 3-6 else
8: Output: Estimate of AAI $\hat{\mathcal{I}} = \mathcal{S}^{(r)}$.

Suppose that we are given an estimate, say $\mathcal{S}^{(1);\mathbf{y}_r,\mathbf{H}_r}$, of the true support and let $L^{(1)} = \mathcal{L}(\mathcal{S}^{(1)}; \mathbf{y}_r, \mathbf{H}_r)$ be the corresponding least-squares loss. We want to transition to another estimate $\mathcal{S}^{(2)}$ that is closer (in terms of the number of true variables), or equal, to $\mathcal{S}^*$, the true support. The SWAP algorithm transitions from $\mathcal{S}^{(1)}$ to an $\mathcal{S}^{(2)}$ in the following manner: Swap every $i \in \mathcal{S}^{(1)}$ with $i \in (\mathcal{S}^{(1)})^C$ and compute the loss $L_{i,i'}^{(1)} = \mathcal{L}\big(\mathcal{S}^{(1)} \backslash i \cup i'; \mathbf{y}_r, \mathbf{H}_r\big)$

If $min_{i,i'} L_{i,i'}^{(1)} < L^{(1)}$, then there exists a support that has a lower loss than $L^{(1)}$. Subsequently, we find $(\hat{i}, \hat{i}') = argmin_{i,i'} L_{i,i'}^{(1)}$ and let $\mathcal{S}^{(2)} = \mathcal{S}^{(1)} \backslash \hat{i} \cup \hat{i}'$. We repeat the above steps to find a sequence of supports $\mathcal{S}^{(1)}, \mathcal{S}^{(2)}, \ldots, \mathcal{S}^{(r)}$ where $\mathcal{S}^{(r)}$ has the

property that $min_{i,i'} L_{i,i'}^{(1)} \geq L^{(r)}$. In other words, we stop SWAP when perturbing $\mathcal{S}^{(r)}$ by one variable increases or does not change the resulting loss.

3.1.2 Selecting the initial support

The main input to SWAP is the initial support $\mathcal{S}^{(1)}$, which also implicitly specifies the desired sparsity level of the estimated support. Recall that n_t is the unknown number of non-zero entries in $\mathbf{x}$. If n_t is known, then SWAP can be initialized using the output of some other sparse regression algorithm. In this way, SWAP can boost the performance of other sparse regression algorithms.

When n_t is not known, which is the case in many applications, SWAP can be easily used in conjunction with other sparse regression algorithms to compute a solution path, i.e., a list of all possible estimates of the support over different sparsity levels. Once a solution path is obtained, model selection methods, such as cross-validation or stability selection [32], can be applied to estimate the support.

3.1.3 Computational complexity

The main computational step in SWAP algorithm is Line 2, where the loss $L_{i,i'}^{(r)}$ is computed for all possible swaps (i, i'). As $n_t = |\mathcal{S}^{(r)}|$ then clearly $n_t(N_t - n_t)$ such computations need to be done in each iteration of the algorithm. Using properties of the orthogonal projection matrix, we have that for any $\mathcal{S}$

$$\Pi[\mathcal{S}] = \Pi[\mathcal{S}\backslash i] + \frac{(\Pi^{\perp}[\mathcal{S}\backslash i]\mathbf{H_i})(\mathbf{\Pi}^{\perp}[\mathcal{S}\backslash \mathbf{i}]\mathbf{H_i})^{\mathbf{T}}}{\mathbf{H_i^T}\mathbf{\Pi}^{\perp}[\mathcal{S}\backslash \mathbf{i}]\mathbf{H_i}}, i \in \mathcal{S} \tag{3.2}$$

To compute $L_{i,i'}^{(r)}$, we need to compute the orthogonal projection matrix $\Pi^{\perp}[\mathcal{S}^{(r)}\backslash i \cup i']$. Once $\Pi^{\perp}[\mathcal{S}^{(r)}\backslash i]$ is computed, $\Pi^{\perp}[\mathcal{S}^{(r)}\backslash i \cup i']$ can be easily computed for all $i' \in (\mathcal{S}^{(r)})^C$, using the above rank one update. Thus, effectively, the computational complexity of Line 2 is roughly $\mathcal{O}(n_t(N_t - n_t)\mathcal{I}_{s-1})$, where $\mathcal{I}_{s-1}$ is the complexity of computing a projection matrix of rank $s - 1$.

3.2 Modified SWAP algorithm

We have modified the SWAP algorithm to accommodate the prior information in GSSK that the non-zero entries in $\mathbf{x}$ are all one. The proposed loss function is

$$\mathcal{L}(\mathcal{S}; \mathbf{y_r}, \mathbf{H_r}) = ||\mathbf{y} - \mathbf{H}(\mathcal{S}).\mathbf{1_{n_t}}||_{\mathbf{2}}^{\mathbf{2}} \tag{3.3}$$

Since, the matrix inversions in (3.1) are not present in (3.3), the computational complexity of modified swap is significantly reduced. An algorithmic description of modified SWAP algorithm is given in Algorithm 2. In general, the iterations of SWAP will be continued until the condition in Step 4 of Modified SWAP fails. However, to reduce the computational complexity, we terminate modified SWAP iterations once the iteration counter r equals max-iter=10.

Algorithm 2 Modified SWAP

1: Inputs: Observation $\mathbf{y}_r$, channel matrix $\mathbf{H}_r$ and initial support $\mathcal{S}^{(1)}$
2: Let $r = 1$ and $L^{(1)} = \mathcal{L}(\mathcal{S}^{(1)}; \mathbf{y_r}, \mathbf{H}_r)$
3: Swap $i \in \mathcal{S}^{(r)}$ with $j \in (\mathcal{S}^{(r)})^C$ and compute the loss $L_{i,j}^{(r)} = \mathcal{L}((\mathcal{S}^{(r)}/i) \cup j; \mathbf{y}_r, \mathbf{H}_r)$
4: if $min_{i,j} L_{i,j}^{(r)} < L^{(r)}$ then perform steps 5-7, else, stop.
5: $\{\hat{i}, \hat{j}\} = \arg\min_{i,j} L_{i,j}^{(r)}$ (In case of a tie, choose a pair arbitrarily)
6: Let $\mathcal{S}^{(r+1)} = (\mathcal{S}^{(r)}/\hat{i}) \cup \hat{j}$ and $L^{(r+1)}$ be the corresponding loss.
7: Let r = r + 1 and repeat steps 3-6 else
8: Output: Estimate of AAI $\hat{\mathcal{I}}$ = $\mathcal{S}^{(r)}$.

which is same as SWAP algorithm except for the change in loss function.

3.3 Proposed two stage GSSK detection framework

Modified SWAP algorithm requires an initial estimate $\mathcal{S}^{(1)}$. One way to generate $\mathcal{S}^{(1)}$ is by randomly sampling without replacement from the set $\{1, \ldots, N_t\}$. However, it was shown in [9] that the performance of SWAP when initialized with the the output of standard algorithms like OMP, BPDN etc. is far superior in comparison with randomly generated initial estimates. This motivate the two stage GSSK detection framework outlined in Algorithm 3 which combine existing GSSK detection algorithms with Modified SWAP algorithm.

Each iteration of modified SWAP requires the computation of $n_t(N_t - n_t)$ l_2 norms

and each norm computation has complexity of order $\mathcal{O}(N_r)$. Hence, the per iteration complexity of modified SWAP is $\mathcal{O}(n_t N_r N_t)$. Further, the number of iterations is fixed at max-iter=10. Hence, the overall complexity of modified SWAP is $\mathcal{O}(n_t N_r N_t)$ which is same as the complexity of OMP and much lower than the $\mathcal{O}(N_t^3)$ complexity of BPDN and CSR. This also implies that complexity of the proposed two stage GSSK detection with OMP in the first stage (OMP-MS) is same as the $\mathcal{O}(n_t N_r N_t)$ complexity of OMP. Likewise, the complexity of the proposed two stage GSSK detection with CSR in the first stage (CSR-MS) is same as the $\mathcal{O}(N_t^3)$ complexity of CSR.

Algorithm 3 Proposed two Stage GSSK detection framework

1: Inputs: Observation $\mathbf{y}_r$, channel matrix $\mathbf{H}_r$.
2: Apply standard GSSK detection schemes like CSR, OMP etc. to produce an initial estimate $\mathcal{S}^{(1)}$ of AAI $\mathcal{I}$.
3: Use Modified SWAP with initial estimate $\mathcal{S}^{(1)}$ to produce the final estimate $\hat{\mathcal{I}}$.

CHAPTER 4

Numerical Simulations

In this section we demonstrate the performance of the proposed two stage framework. We consider GSSK systems with different sets of (N_t, N_r, n_t) and different channel conditions outlined in *chapter 2* . The figures present estimates of BER after performing 10^4 iterations and in each iteration, the channel, transmitted signal and noise are randomly generated.

Here, the performance of the proposed framework with different approaches in the first stage and modified SWAP as second stage is illustrated. In the first stage, OMP, convex superset selection (CSS) and fast bayesian matching pursuit (FBMP) are used. CSS and FBMP are supposedly robust to correlations among columns of observation matrix unlike OMP, however these are computationally more complex compared to OMP. Hence in the following results, modified SWAP induces more improvement for OMP compared to CSS and FBMP.

In the following figures, OMP, CSS and FBMP denotes BER curves with only the respective algorithms used for GSSK detection. OMP-MS, CSS-MS and FBMP-MS denotes the BER curves for the proposed framework with the respective algorithms used in the first stage and modified SWAP in the second stage. Expo and block refers to the cases when the correlation matrix has exponential form and block diagonal form respectively.

$R_t x$ and $R_r x$ denotes the transmitter and receiver correlation matrices respectively.

4.1 Channel Model 1: $\mathbf{H}_{i,:} \sim \mathcal{CN}(\mathbf{0}_{N_t}, \mathbf{\Sigma})$

Fig. 4.1-Fig. 4.2 plot the SER of proposed two stage framework for a GSSK system with $N_t = 32, N_r = 16$ and $n_t = 3$ when the correlation factor ρ in $\mathbf{\Sigma}_{i,j} = \rho^{i-j}$ increases from $\rho = 0$ to $\rho = 0.8$.

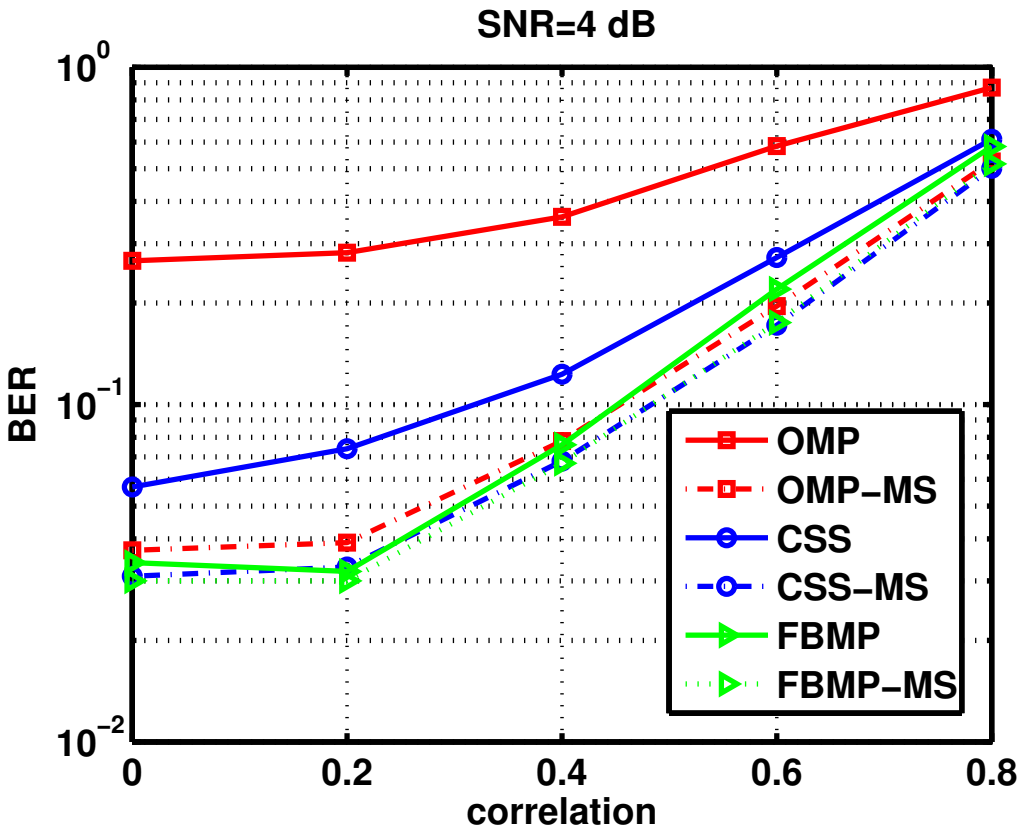

Figure 4.1: case (4.1): Correlation Vs Bit error Rate for SNR=4 dB, $N_t = 32$, $N_r = 16$ and $n_t = 3$.

Fig. 4.1 shows Correlation vs Bit Error Rate curves for OMP and OMP followed by Modified SWAP for SNR=4 dB. As shown the improvement in OMP is is significant compared to the other algorithms. As other algorithms are better in performance compared to OMP the improvement is also seen to be less. Almost linear increase in BER with respect to correlation can be observed. A shift in curves is observed for higher SNR values as shown in Fig. 4.2.

4.2 Kronecker channel model with receiver correlation matrix assumed to be Identity matrix

When the receiver correlation matrix is assumed to be identity matrix, i.e., assuming that the correlation between the links is present only on the transmitter side, the plot of BER vs correlation is still found to have significant improvement both for OMP and CSR. FBMP seems to improve lesser in comparison to the other algorithms. This is

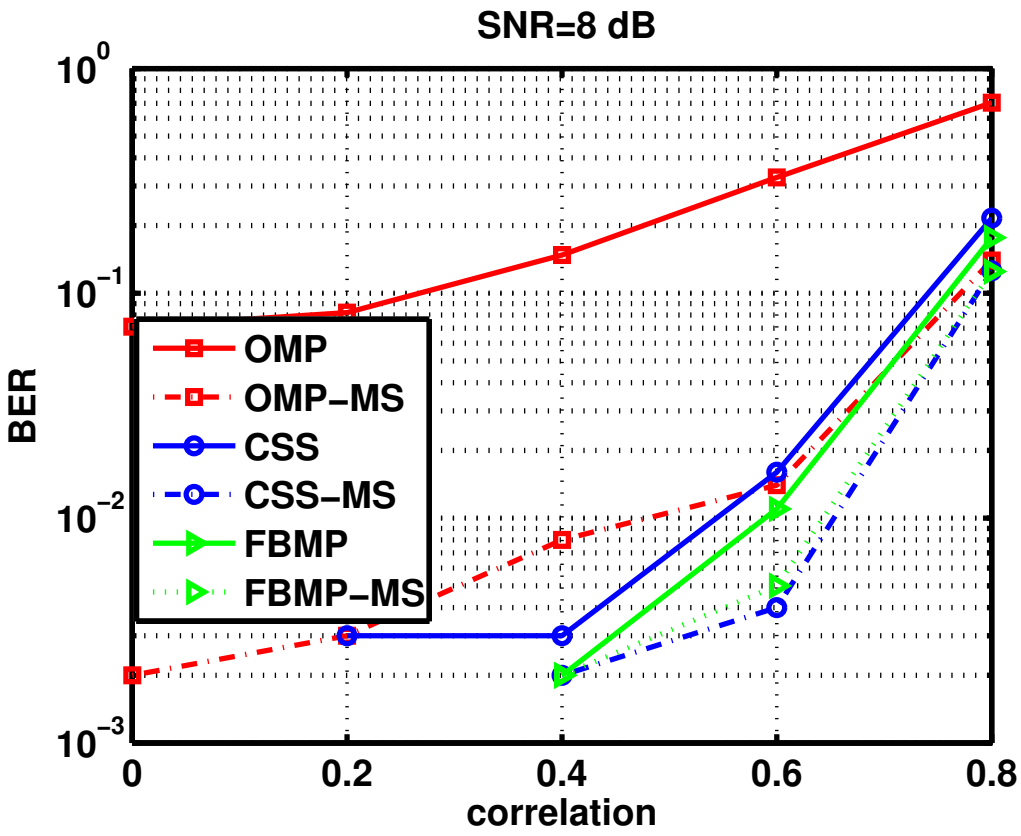

Figure 4.2: case (4.1):Correlation Vs Bit error Rate for SNR=8 dB $N_t = 32$, $N_r = 16$ and $n_t = 3$.

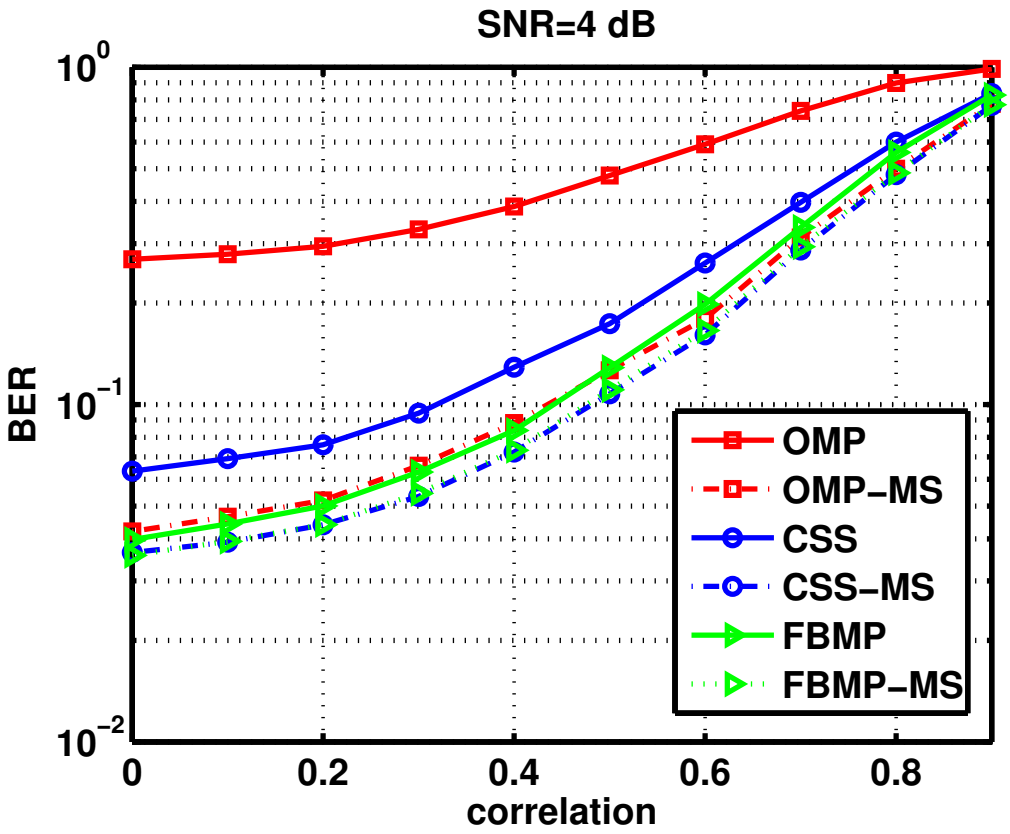

Figure 4.3: case (4.2): Correlation Vs Bit error Rate for SNR=4 dB$N_t = 32$, $N_r = 16$ and $n_t = 3$.

shown in Fig.4.3 and Fig. 4.4 for different SNR values.

4.3 Kronecker channel model with transmitter and receiver correlation matrices are arbitrary

Fig. 4.5 and Fig. 4.6 compares the performance of proposed framework assuming the correlation between links exist on both transmitter and receiver ends. The improvement after second stage for all the algorithms is found to drop as compared to the previous channel model ($R_{rx} = I$). Similar to the previous cases there is shift in BER curves as SNR is increased as shown in Fig.4.6.

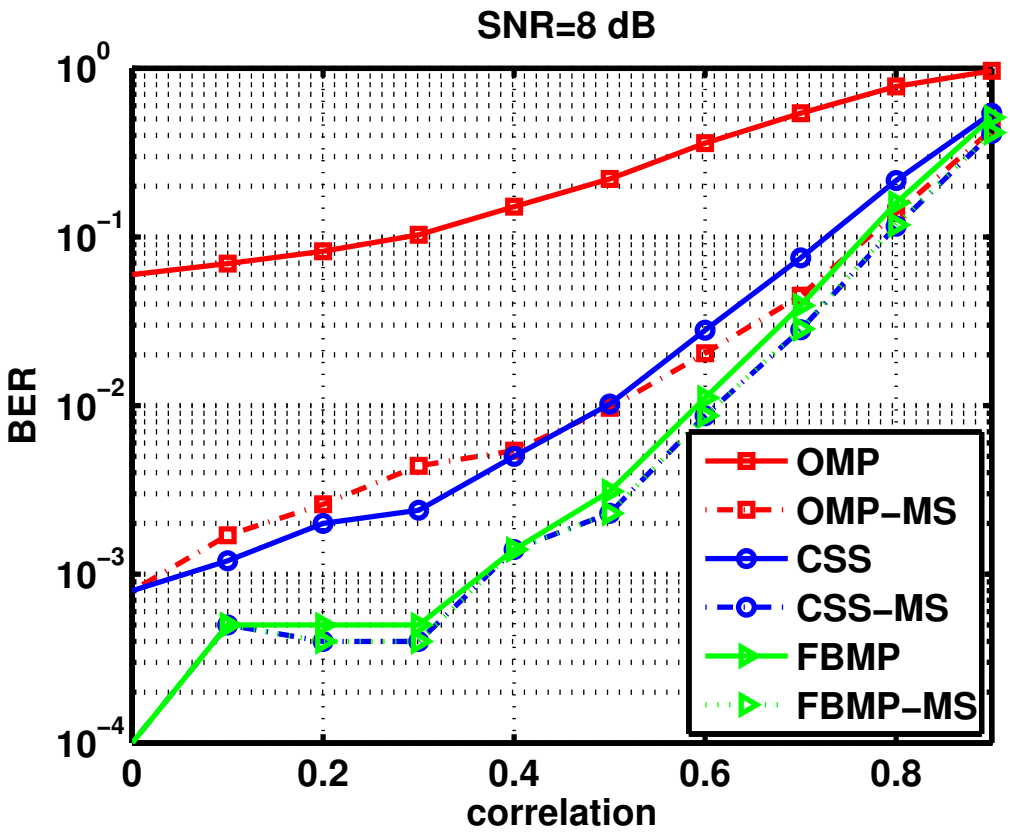

Figure 4.4: case (4.2):Correlation Vs Bit error Rate for SNR=8 dB, $N_t = 32$, $N_r = 16$ and $n_t = 3$.

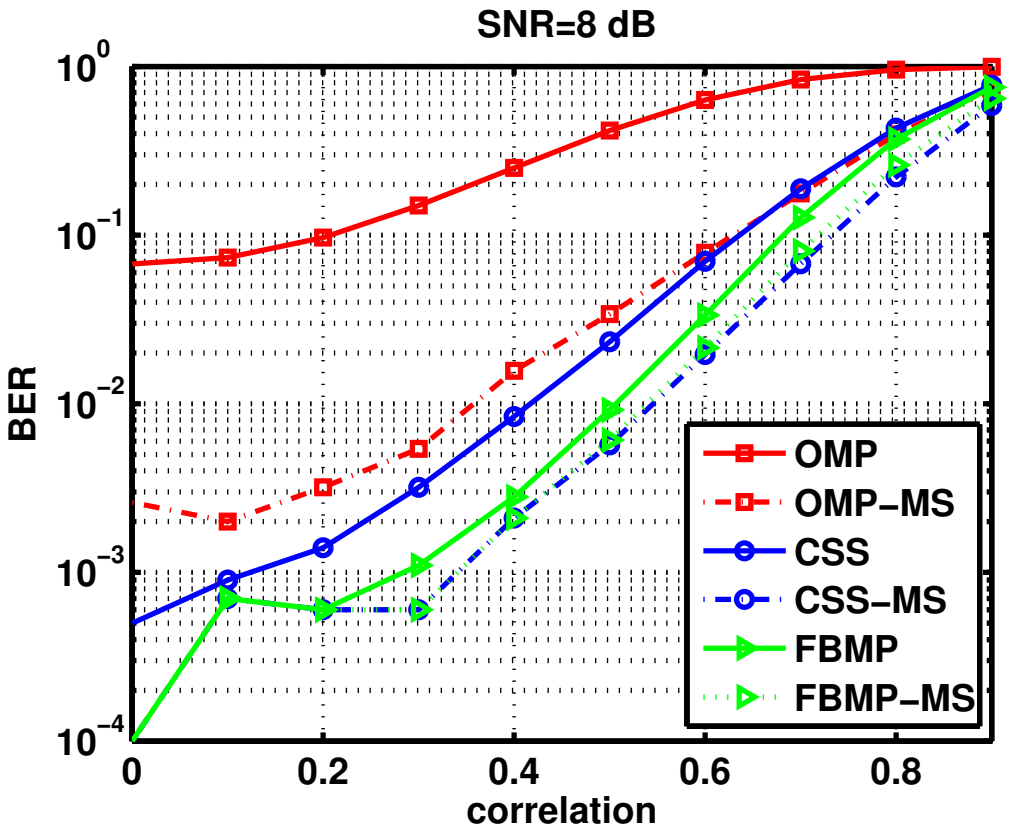

Figure 4.5: case (4.3):Correlation Vs Bit error Rate for SNR=8 dB.

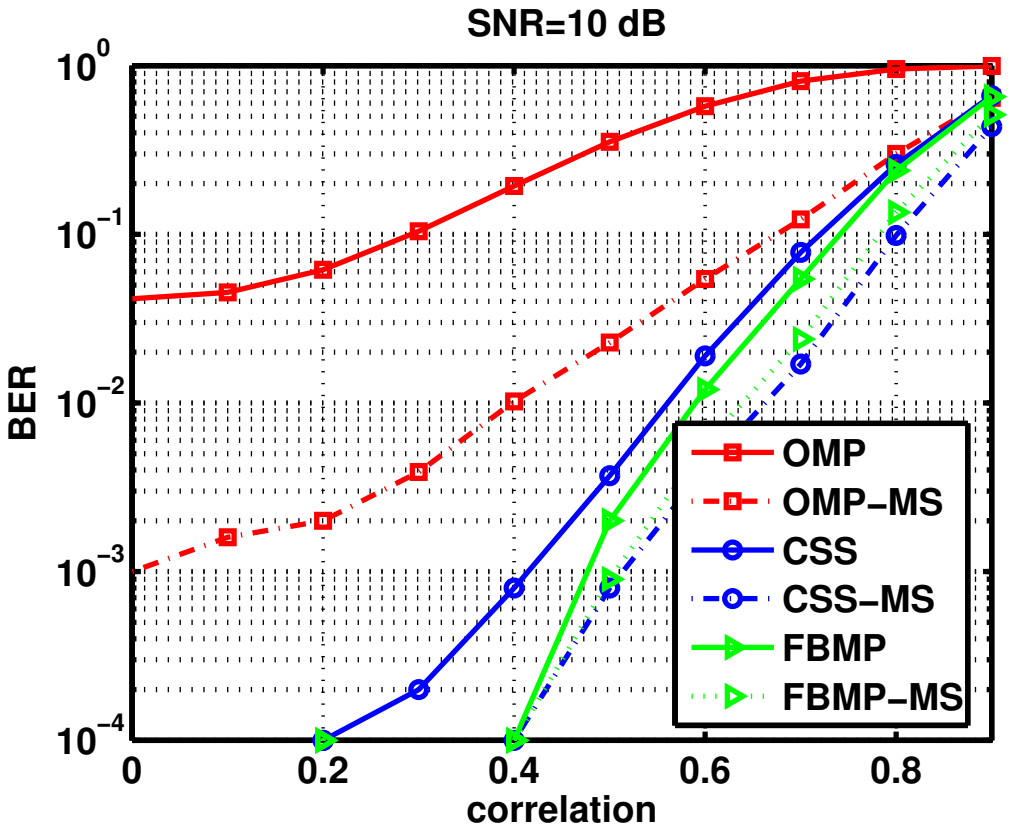

Figure 4.6: case (4.3): Correlation Vs Bit error Rate for SNR=10 dB.

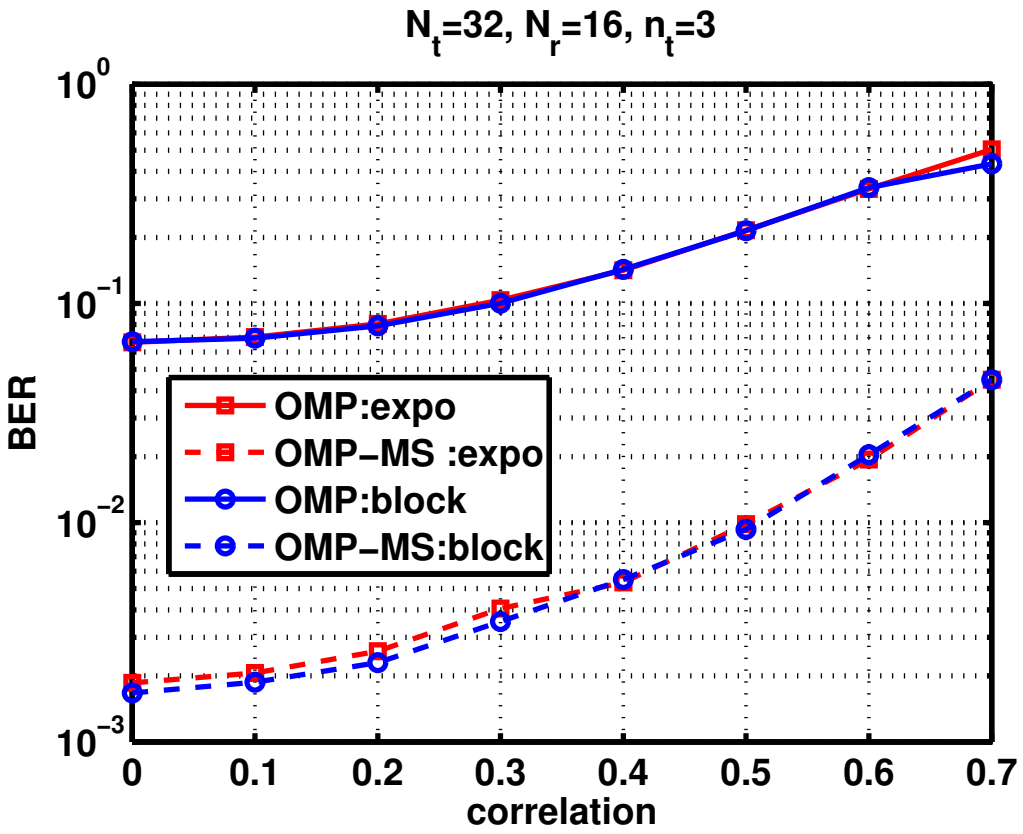

Figure 4.7: case(4.4):BER vs correlation curve for exponential and block diagonal correlation $N_t = 32$, $N_r = 16$ and $n_t = 3$,SNR=8 dB.

4.4 Channel Model: $\mathbf{H}_{i,:} \sim \mathcal{CN}(\mathbf{0}_{N_t}, \mathbf{\Sigma})$ where Σ is block diagonal matrix

As described in 2 the channel model has Σ matrix in block diagonal form. Each antenna is correlated only to adjacent 3(say) antennas on either side. The correlation decreases exponentially to either sides.

The BER vs correlation plot shown in Fig.4.7 is for $N_t = 32$, $N_r = 16$ and $n_t = 3$.

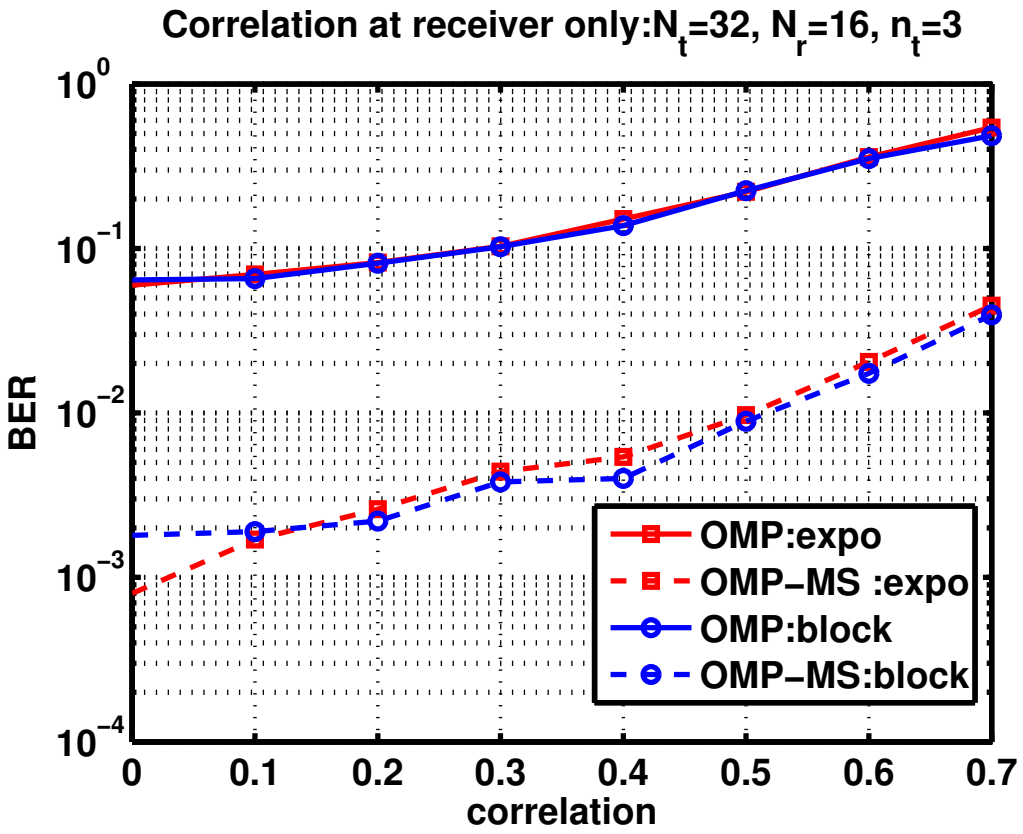

Figure 4.8: case(4.5):Comparison between exponential and block diagonal form for R_{tx} and and $R_{rx} = I$ $N_t = 32$, $N_r = 16$ and $n_t = 3$, SNR=8 dB.

4.5 Kronecker channel model with R_{tx} in block diagonal form and R_{rx} as identity matrix

In this section we have used the same Kronecker channel model but the transmitter channel matrix following a block diagonal form (as in Channel Model 3 in chapter 2) and correlation between links is assumed to be absent at the receiver. Fig. 4.8 shows the BER plots for OMP and OMP followed by modified SWAP at SNR = 8 dB. Here $N_t = 32$, $N_r = 16$ and $n_t = 3$. The results are also compared with the Kronecker model with exponential correlation between antennas. The results are almost same.

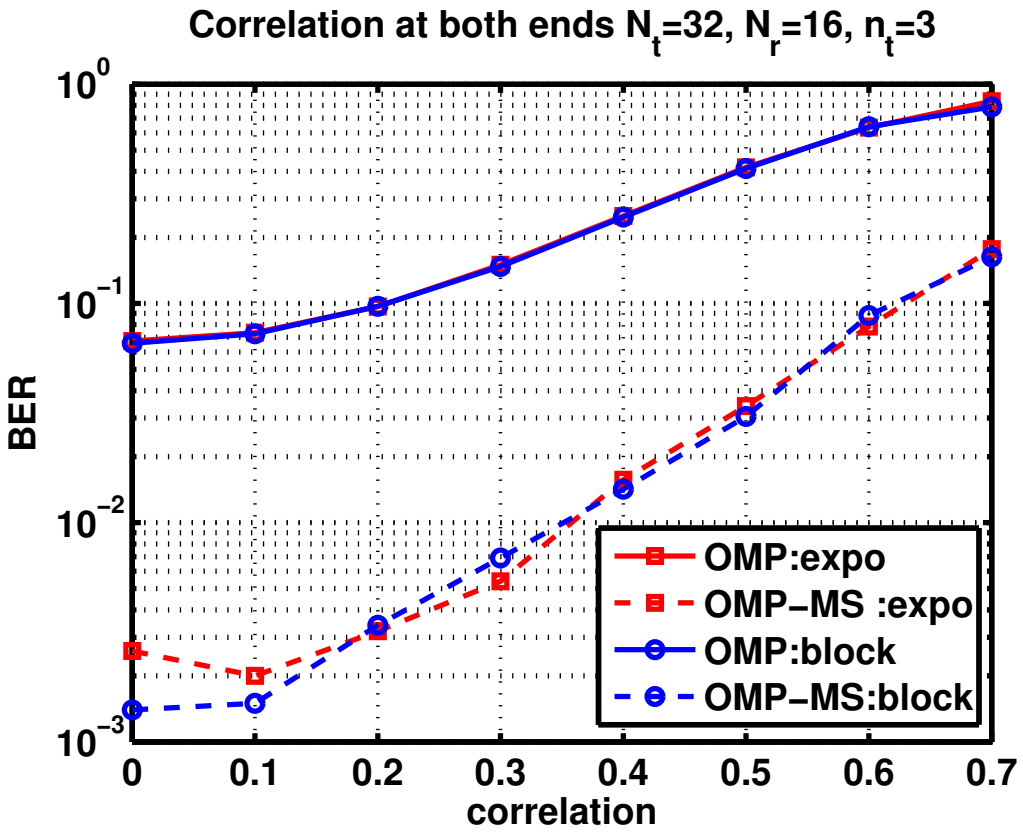

Figure 4.9: case(4.6):Comparison between cases when exponential/block diagonal correlation exists at both transmitter and receiver ends $N_t = 32$, $N_r = 16$ and $n_t = 3$, SNR=8 dB.

4.6 Kronecker channel model with both R_{tx} and R_{rx} in block diagonal form

In this section we have used the same Kronecker channel model but the transmitter channel matrix and receiver channel matrix following a block diagonal form (as in Channel Model 3) . Fig. 4.9 shows the BER plots for OMP and OMP followed by modified SWAP at SNR = 8 dB. Here $N_t = 32$, $N_r = 16$ and $n_t = 3$. The results are also compared with the Kronecker model with exponential correlation between antennas. The results are found to be almost same.

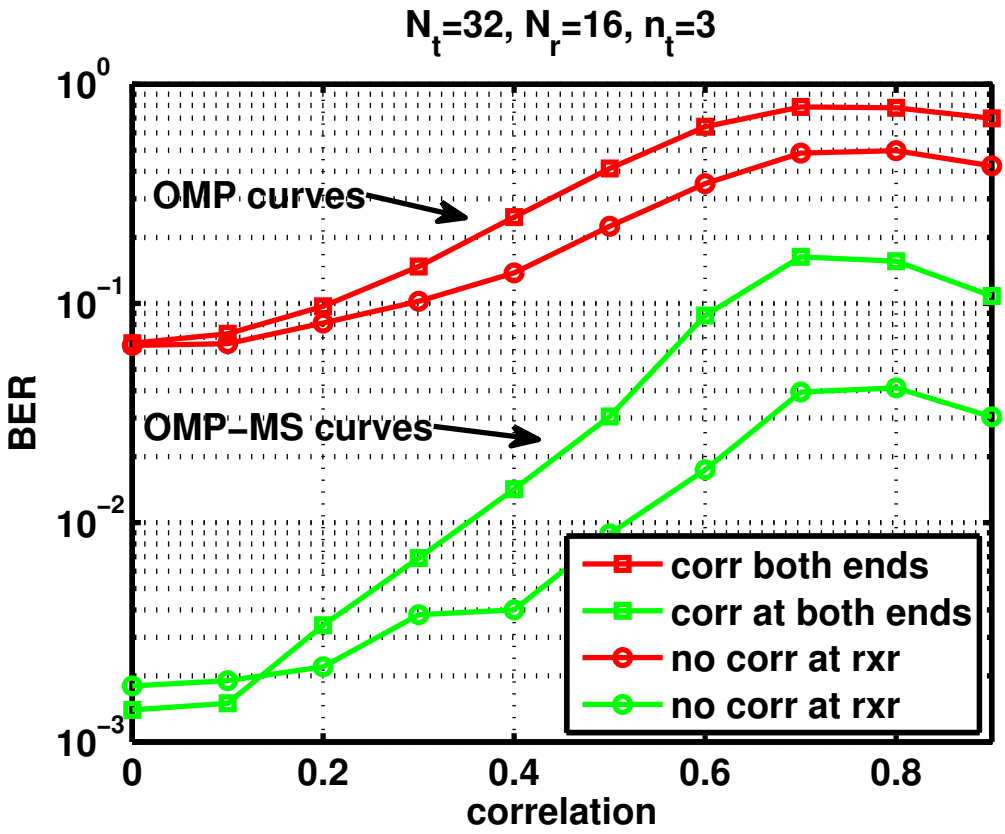

Figure 4.10: case(4.7): Comparison between cases when block diagonal form is used for (1) both R_{tx} and R_{rx}, (2) only R_{tx} and $R_{rx} = I$ for $N_t = 32$, $N_r = 16$ and $n_t = 3$, SNR=8 dB.

4.7 Comparison of Kronecker channel with and without correlation at receiver

In this section we analyze the Kronecker channel model with correlation at both ends Vs no correlation at receiver. Both the transmitter channel matrix and receiver channel matrix follow a block diagonal form (as in Channel Model 3) . Fig. 4.10 shows the BER plots for OMP and OMP followed by modified SWAP at SNR = 8 dB. Here $N_t = 32$, $N_r = 16$ and $n_t = 3$. The results shows the obvious, BER degrades as there is correlation at both ends both for OMP and OMP-MS.

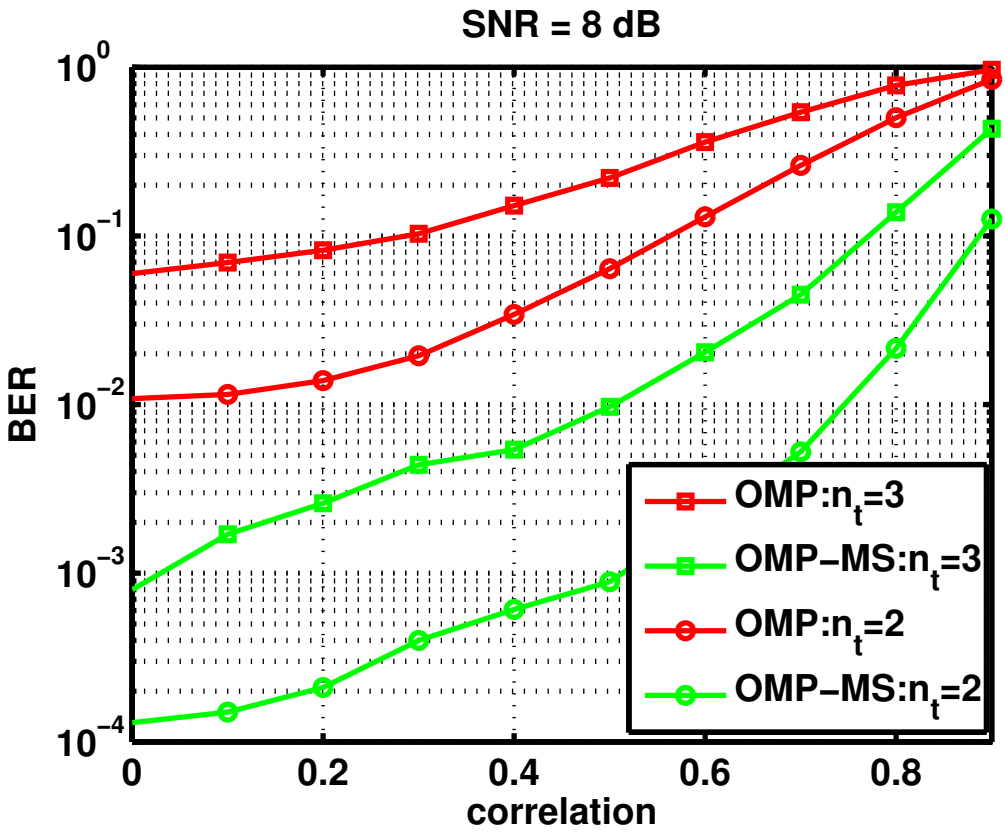

Figure 4.11: case(4.8): Comparison between cases when block diagonal form is used for only R_{tx} and $R_{rx} = I$ for $N_t = 32$, $N_r = 16$ and SNR=8 dB.

4.8 Performance of Modified SWAP for settings with different number of active antennas

In this section we analyze the Kronecker channel model with no correlation at receiver. Fig. 4.11 shows the BER plots for OMP and OMP followed by modified SWAP at SNR = 8 dB. Here $N_t = 32$, $N_r = 16$ and $n_t = 3$. The results shows that BER improves when there are lesser number of active antennas both for OMP and OMP-MS. The algorithm is able to recover exact locations with higher probability when number of active antennas are less.

4.9 Performance of Modified SWAP with respect to SNR

The Performance of OMP and OMP followed by modified SWAP are shown in Fig. 4.12. As SNR increases both curves move down showing a decrease in BER. Since

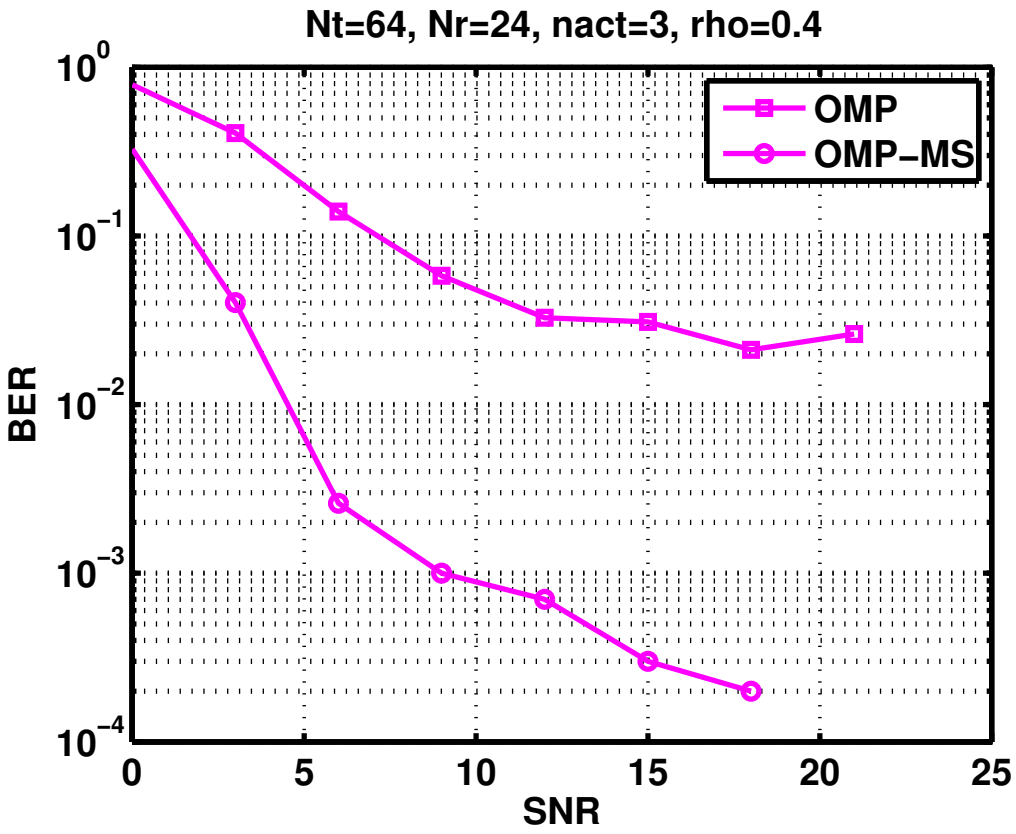

Figure 4.12: case(4.9): BER vs SNR

there is correlation existing given by ρ value 0.4, the gap between two curves becomes larger as SNR increases

4.10 Comparison of Time Complexity

The runtime of the algorithms are shown in Fig. 4.13. The number of transmitting antennas are taken as double the number of receiving antennas. The runtime increases with number of antennas for all algorithms. CSR is shown to take much larger time compared to OMP. OMP followed by Modified SWAP and CSR followed by SWAP takes almost the same amount of time as OMP and CSR themselves. So Modified SWAP improves the performance without much overhead in time taken. Also as seen from the previous figures as well, OMP followed by Modified SWAP performs as good as CSR without taking as much time as CSS.

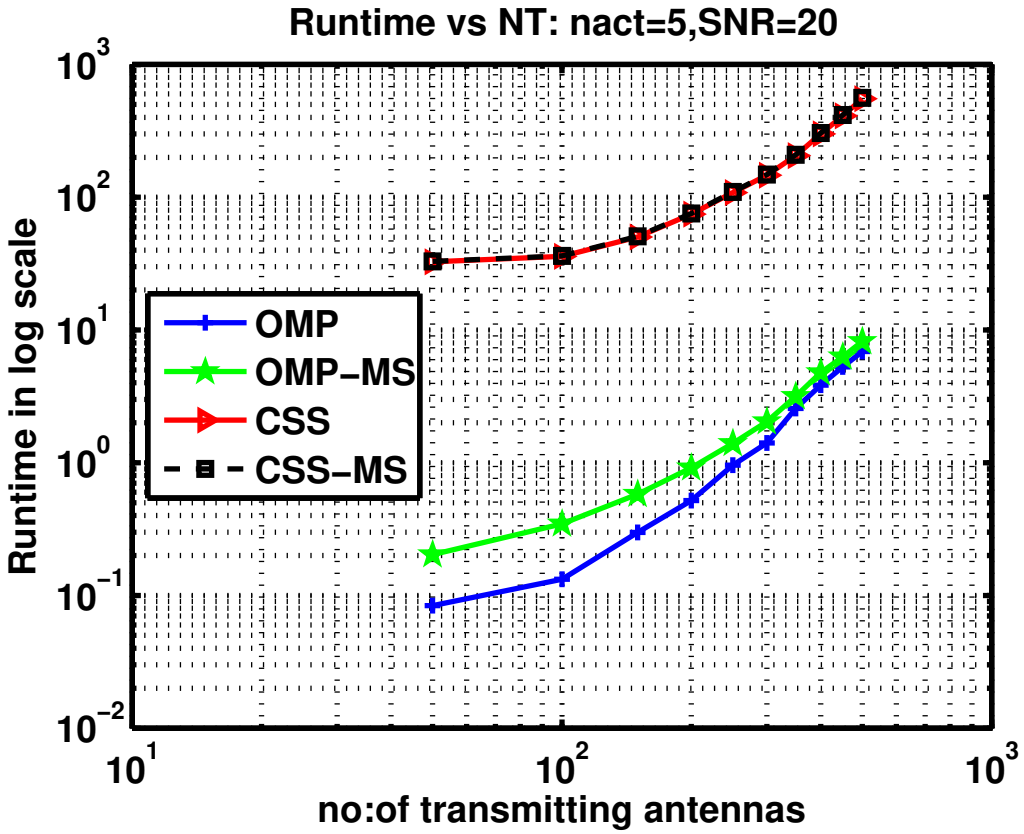

Figure 4.13: case(4.10): Runtime vs Number of transmitting antennas

CHAPTER 5

Conclusions and Future work

Considering the application of generalized space shift keying (GSSK), a novel CS based detection framework for improving performance of various applications with correlated design matrices is proposed. The proposed framework involves any simple CS algorithm as first stage which is followed by Modified SWAP. The second stage involving Modified SWAP brings about significant improvement in BER without much increase in time complexity. Numerical simulations indicate that the proposed framework can significantly improve the performance of existing CS based schemes with a very modest increase in the computational complexity even when the channel model is highly correlated.

The same algorithm can be extended to improve the performance of generalized spatial modulation (GSM). In GSM both antenna indices and the symbols transmitted convey information. However, the symbols transmitted belong to a finite alphabet rather than real numbers. So this prior information of finite alphabet can be used in implementing SWAP for GSM detection. Again the complexity can be reduced as there will be no complex inversions.

REFERENCES

[1] J. Haupt, W. U. Bajwa, G. Raz, and R. Nowak, "Toeplitz Compressed Sensing Matrices With Applications to Sparse Channel Estimation," vol. 56, no. 11, pp. 5862–5875, 2010.

[2] T. Cai and T. Jiang, "Limiting laws of coherence of random matrices with applications to testing covariance structure and construction of compressed sensing matrices."

[3] R. Giryes and M. Elad, "OMP with highly coherent dictionaries," *10th Int. Conf. on Sampling Theory Appl.(SAMPTA)*, vol. 2, no. 1, pp. 9–12, 2013.

[4] C. H. Wu, W. H. Chung, and H. W. Liang, "OMP-based detector design for space shift keying in large MIMO systems," *2014 IEEE Global Communications Conference, GLOBECOM 2014*, no. Ml, pp. 4072–4076, 2014.

[5] A. Fannjiang and W. Liao, "Coherence Pattern Guided Compressive Sensing with Unresolved Grids âĹŮ," vol. 5, no. 1, pp. 179–202, 2012.

[6] Z. Zhang, S. Member, and B. D. Rao, "Sparse Signal Recovery with Temporally Correlated Source Vectors Using Sparse Bayesian Learning," pp. 1–15, 2011.

[7] G. Chen, A. Divekar, and D. Needell, "Guaranteed sparse signal recovery with highly coherent sensing matrices," pp. 1–16, 2014.

[8] Z. Gao, L. Dai, C. Qi, C. Yuen, and Z. Wang, "Near-Optimal Signal Detector Based on Structured Compressive Sensing for Massive SM-MIMO," vol. 66, no. 2, pp. 1860–1865, 2017.

[9] D. Vats and R. Baraniuk, "Swapping Variables for High-Dimensional Sparse Regression from Correlated Measurements," pp. 1–36, 2013.

[10] B. Peter, "Correlated variables in regression : clustering and sparse estimation," pp. 1–40, 2012.

[11] S. Reid, "Sparse regression and marginal testing using cluster prototypes," pp. 364–376, 2016.

[12] B. Ghorbani, "Sparse Regression with highly correlated Predictors," pp. 1–15.

[13] C.-M. Yu, S.-H. Hsieh, H.-W. Liang, C.-S. Lu, W.-H. Chung, S.-Y. Kuo, and S.-C. Pei, "Compressed Sensing Detector Design for Space Shift Keying in MIMO systems," *IEEE Commun. Lett.*, vol. 16, no. 10, pp. 1556–1559, Oct 2012.

[14] C.-H. Wu, W.-H. Chung, and H.-W. Liang, "OMP-based Detector Design for Space Shift Keying in Large MIMO Systems," in *Proc. IEEE GLOBECOM*, Dec 2014, pp. 4072–4076.

[15] L. He, J. Wang, W. Ding, and J. Song, "l_∞ Minimization Based Symbol Detection for Generalized Space Shift Keying," *IEEE Commun. Lett.*, vol. 19, no. 7, pp. 1109–1112, July 2015.

[16] W. Liu, N. Wang, M. Jin, and H. Xu, "Denoising Detection for the Generalized Spatial Modulation System Using Sparse Property," *IEEE Commun. Lett.*, vol. 18, no. 1, pp. 22–25, Jan 2014.

[17] R. Y. Chang, W. H. Chung, and S. J. Lin, "Detection of space shift keying signaling in large MIMO systems," *IWCMC 2012 - 8th International Wireless Communications and Mobile Computing Conference*, pp. 1185–1190, 2012.

[18] C. Toglia, D. Kettler, F. Kennedy, and S. Dubowsky, "A Stochastic MIMO Radio Channel Model with Experimental Validation," vol. 20, no. 6, pp. 3031–3036, 2009.

[19] D. Chizhik, J. Ling, P. Wolniansky, R. Valenzuela, N. Costa, and K. Huber, "Multiple-input - multiple-output measurements and modeling in Manhattan," *IEEE Journal on Selected Areas in Communications*, vol. 21, no. 3, pp. 321–331, 2003.

[20] M. D. Renzo and H. Haas, "Space Shift Keying (SSK) MIMO over Correlated Rician Fading Channels: Performance Analysis And a New Method for Transmit-Diversity," *IEEE Transactions on Communications*, vol. 59, no. 1, pp. 116–129, 2011.

[21] M. Koca and H. Sari, "A General Framework for Performance Analysis of Spatial Modulation over Correlated Fading Channels," vol. 58, no. 9, pp. 2590–2603, 2011.

[22] M. D. Renzo and H. Haas, "Bit Error Probability of Spatial Modulation SM-MIMO over Generalized Fading Channels," vol. 61, no. 3, pp. 1124–1144, 2012.

[23] D. N. Alotaibi. (2017) Exploiting indices of silent antennas to increase the spectral efficiency of ssk. [Online]. Available: https://www.slideshare.net/NafelAlotaibi/exploiting-indices-of-silent-antennas-to-increase-the-spectral-efficiency-of-ssk

[24] V. A. Aalo, "Performance of Maximal-Ratio Diversity Systems in a Correlated Nakagami-Fading Environment," vol. 43, no. 8, pp. 2360–2369, 1995.

[25] J. Jeganathan and A. G. L. Szczecinski, "Generalized space shift keying modulation for mimo channels," *Published in: Personal, Indoor and Mobile Radio Communications, 2008. PIMRC 2008. IEEE 19th International Symposium on*, Sept 2008.

[26] J. Jeganathan, A. Ghrayeb, S. Member, L. Szczecinski, S. Member, and A. Ceron, "Space Shift Keying Modulation for MIMO Channels," vol. 8, no. 7, pp. 3692–3703, 2009.

[27] A. Garcia-rodriguez and C. Masouros, "Low-Complexity Compressive Sensing Detection for Spatial Modulation in Large-Scale Multiple Access Channels," vol. 63, no. 7, pp. 2565–2579, 2015.

[28] X. Zhang, Q. Liu, and M. Jin, "Detection of Generalized Space Shift Keying Signal with Sparse Reconstruction," vol. XX, no. XX, pp. 1–5, 2016.

[29] H. Kim, J. Lee, and Y. H. Lee, "Maximum a Posteriori OMP Detection for Generalized Space Shift Keying," pp. 0–5, 2016.

[30] A. D. Ssk, "Optimal Power Allocation for Space Shift Keying Modulation in a Distributed Antenna System," vol. 17, pp. 1734–1737, 2013.

[31] C. Soussen, "Representations With Partial Support Information," vol. 59, no. 11, pp. 7509–7524, 2013.

[32] N. Meinshausen, "Stability selection," pp. 417–473, 2010.